Materials Research Express

RECEIVED
25 October 2016

REVISED
24 January 2017

ACCEPTED FOR PUBLICATION
21 February 2017

PUBLISHED
15 March 2017

PAPER

Reciprocal space mapping study of CdTe epilayer grown by molecular beam epitaxy on (2 1 1)B GaAs substrate

Mustafa Polat, Ozan Arı, Orhan Öztürk and Yusuf Selamet
Department of Physics, Izmir Institute of Technology, Izmir, 35430, Turkey
E-mail: mustafapolat@iyte.edu.tr

Keywords: CdTe/(2 1 1)B GaAs, reciprocal space map, dislocation, shear strain, lattice mismatch, tilting

Abstract
We examine high quality, single crystal CdTe epilayer grown by molecular beam epitaxy (MBE) on (2 1 1)B GaAs substrate using both positions and full width at half maximums (FWHMs) of reciprocal lattice points (RLPs). Our results demonstrate that reciprocal space mapping (RSM) is an effective way to study the structural characteristics of the high-index oriented epitaxial thin films having a large lattice mismatch with the substrate. The measurement method is defined first, and then the influence of shear strain (ϵ_{xz}) on the position of the (5 1 1) node of epilayer is clarified. It is concluded that the lattice tilting is likely to be related with the lattice mismatch. Nondestructive measurement of the dislocation density is achieved by applying the mosaic crystal model. The screw dislocation density, estimated to be 7.56×10^7 cm^{-2}, was calculated utilizing the broadened peakwidths of the asymmetric RLP of the epilayer lattice.

1. Introduction

Reciprocal space mapping (RSM) has been widely utilized to find out the microstructure and deviations from ideal crystal structures, present in materials ranging from polycrystalline to single-crystalline [1]. RSM can deliver further structural information as compared to conventional methods such as rocking curve (RC) scan due to its two-dimensional (2D) characteristics [2]. This particularly provides a significant advantage when applied to epitaxial thin films having large lattice mismatches. Nondestructive measurement of the threading-dislocation (TD) densities, for instance, relies on prediction of individual parameters, such as domain tilt and twist, of a mosaic layer structure [3]. In addition to the large lattice mismatch, some epitaxial heterostructures have also the low-symmetry surface characteristics. CdTe/(2 1 1)B GaAs is obviously one of the outstanding examples of these types of structures. Structural analysis of the high-index oriented zinc-blende epitaxial layers when combined with the large lattice mismatch becomes much more challenging. Furthermore, the surface normal of epilayer lattice tilts approximately 3° with respect to that of substrate [4]. Each one of these factors make the structure being examined extremely difficult to analyze, especially with the traditional x-ray diffraction (XRD) methods. As a result, a limited number of studies so far have been dedicated to understanding the structural properties of this heterostructure [5–8]. The common point of all these studies is that they were carried out in real space. However, one advantageous option can be mapping in reciprocal space to characterize such heterostructures. At present, the technique has been separately applied to the high-index orientation [9] or to the large lattice mismatched heterostructures [10].

In this letter, the RSM technique is effectively employed to study the lattice tilting, the lattice mismatches, the shear strain produced by the low-symmetry surface and the screw dislocation density of CdTe epilayer grown on (2 1 1) oriented GaAs substrate.

2. Experimental procedure

2.1. Molecular beam epitaxy (MBE) growth of CdTe

The growth details were similar to those described elsewhere [11, 12]. Briefly, CdTe epilayer was grown by molecular beam epitaxy (MBE) system operated in a class 1000 cleanroom environment on a 3-inch epi-ready, semi-insulating (2 1 1)B GaAs wafer after thermal stripping of the oxide layer. Initially, a nucleation layer also

© 2017 IOP Publishing Ltd

Table 1. Experimental positions (Q_x and Q_z) and widths of the peaks (ΔQ_x and ΔQ_z) of measured nodes of CdTe epilayer.

RLPs[a]	Q_x(Å^{-1})	ΔQ_x(Å^{-1})	Q_z(Å^{-1})	ΔQ_z(Å^{-1})
(4 2 2)	−299[b]	1.65	5813	0.72
(5 1 1)	−2355[b]	1.36	5707	0.70

[a] All numbers are given here in the rlu ($\times 10^{-4}$).
[b] The minus sign stands for the [1 $\bar{1}$ $\bar{1}$] direction.

composed of CdTe, was deposited at temperature of 210 °C, then annealed at 400 °C. After that, CdTe growth was initiated at about 300 °C, and maintained for 120 min. The growth was suspended to implement *in situ* cyclic annealing steps under a Te_2 flux at temperature of 400 °C every 120 min. A total of 6 growth/anneal cycles were carried out, and 7.6 μm-thick CdTe epilayer was grown for this study.

2.2. Quality of as-grown CdTe thin films

Full width at half maximum (FWHM) and atomic force microscopy (AFM) roughness were deduced to be 70 arcsec and 4.1 nm, respectively, for the sample being analyzed in this study. On the other hand, measured etch pit density values (EPD) were estimated in the 1×10^7 cm^{-2} and 2×10^8 cm^{-2} range for our different samples with the help of chemical etching [13]. Moreover, according to Raman spectroscopy, transverse optical (TO) and longitudinal optical (LO) phonon modes of as-grown CdTe thin films were acquired at 145.5 cm^{-1} and 169.4 cm^{-1} for our different samples, respectively [13]. In our previous study [14], we showed that the surface roughness can be determined by the relationship between *ex situ* spectroscopic ellipsometry (SE) data and atomic force microscopy (AFM) roughness without constructing any optical model.

2.3. High resolution x-ray reciprocal space mapping (RSM)

The RSM was performed using Philips MRD x-ray diffractometer equipped with a four-fold (2 2 0) Ge monochromator to deliver Cu $K_{\alpha 1}$ x-rays ($\lambda = 0.154\,06$ nm). The x-ray beam direction was aligned with the direction of the [$\bar{1}$ 1 1] of the substrate. Scattered x-rays were detected by a Xe-filled gas proportional counter. In addition, we utilized a three-fold (2 2 0) Ge analyzer on the diffracted beam side to reach high resolution triple axis (TA) configuration. Hence, the acceptance angle of the detection was reduced to approximately 12 arcsec. The radial scans ($\omega - 2\theta$) with omega (ω) scans were combined to create 2D maps in reciprocal space. The (4 2 2) and the (5 1 1) reciprocal lattice points (RLPs) were measured at the center of the sample to minimize the effect of the residual stress [7]. Table 1 contains the positions and FWHMs of the (4 2 2) and the (5 1 1) nodes of CdTe epilayer, and the RLPs are shown in figure 1.

3. Results and discussion

3.1. Lattice tilting

The RLPs along the growth direction can be utilized to quantify the direction and magnitude of tilting of epilayer lattice relative to that of the substrate lattice [15]. In our case, both of these lattices have only a single Bragg reflection along the growth direction as a result of the reflection condition for the zinc-blende crystal structure and the high-index characteristic of the structure. Furthermore, the substrate and epilayer peaks are widely separated due to the large lattice mismatch (14.66%). All RLPs of both lattices were therefore measured separately in the diffraction plane parallel to the (0$\bar{1}$1) crystal plane. The lattice tilting relative to the theoretical reciprocal lattice (RL) axes, also known as the diffractometer axes, was then formulated from simple geometrical consideration of the (4 2 2) nodes (see figure 2). The lattice tilting is found with the help of the following expression:

$$\alpha = \tan^{-1}\left(\frac{Q_x}{Q_z}\right) \tag{1}$$

where Q_x and Q_z are the coordinates of the (4 2 2) node of the epilayer in the directions of [1 $\bar{1}$ $\bar{1}$] and [2 1 1], respectively, and α is the tilt angle. It should be noted that the direction of the tilting can be estimated directly from the movement of the node with respect to those theoretical axes. The calculated value of the tilting (table 2) utilizing the above formula is in good agreement with a previous study carried out in the real space [16]. It was reported that the compressive stress in the earlier stage of growth near the interface leads to a tilt in the (2 1 1) CdTe epilayer [16].

3.2. Out-of-plane lattice mismatch

The exact positions of Q_z components of the (4 2 2) nodes are utilized to calculate the out-of-plane ($m_\perp$) lattice mismatch in general [9]. However, Q_z component of the epilayer lattice moves towards the direction of [$\bar{2}$ $\bar{1}$ $\bar{1}$] according to figure 2 as a result of the lattice tilting. Here, we focused on the scattering vector lengths, denoted by $|\mathbf{q}|$, instead of using the shifted Q_z components. Once the scattering vector magnitudes are determined from

Figure 1. (a) The (4 2 2) and (b) the (5 1 1) nodes of CdTe epilayer. Elongation of these RLPs can be indication of the formation of a mosaic layer structure. The calculated lattice parameters ($a_{\perp}$ and $a_{||}$) are also seen in their insets, with measurements in angstroms (Å).

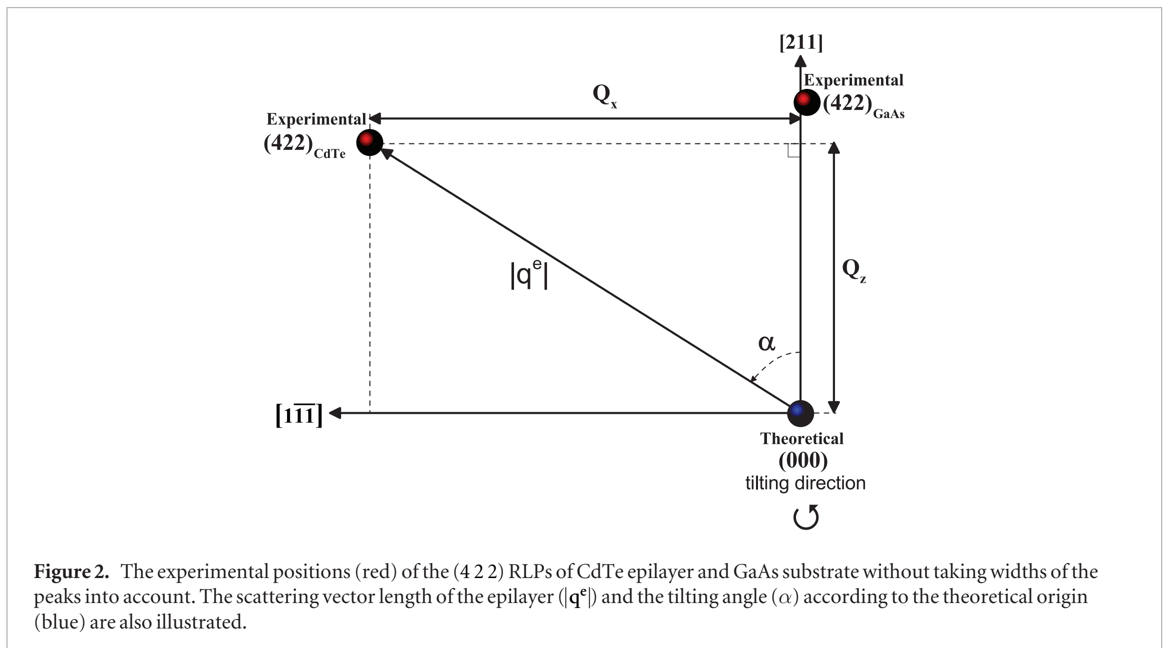

Figure 2. The experimental positions (red) of the (4 2 2) RLPs of CdTe epilayer and GaAs substrate without taking widths of the peaks into account. The scattering vector length of the epilayer ($|\mathbf{q}^{\mathrm{e}}|$) and the tilting angle (α) according to the theoretical origin (blue) are also illustrated.

$|\mathbf{q}| = \sqrt{Q_x^2 + Q_z^2}$, $m_{\perp}$ may be extracted from these $|\mathbf{q}|$ vectors [17]. The way to do this is to overlap the scattering vector of epilayer lattice to that of substrate by means of the calculated tilt angle as follows:

$$m_{\perp} = \frac{a_{\perp} - a_s}{a_s} = \frac{|\mathbf{q}^{\mathrm{s}}| - |\mathbf{q}^{\mathrm{e}}|\cos(\alpha)}{|\mathbf{q}^{\mathrm{e}}|\cos(\alpha)} \tag{2}$$

Table 2. Calculated results utilizing experimental positions and widths of the peaks of the (4 2 2) and the (5 1 1) nodes of CdTe epilayer. In this table, α $m_\perp$, Ψ and $m_\parallel$ represent the lattice tilting, the out-of-plane lattice mismatch, the shear angle and the in-plane lattice mismatch, respectively. $L_\parallel$, β and N_s are the lateral coherence length, the domain tilt and the screw dislocation density, respectively.

α	2.99	(°)	$L_\parallel$	2973	(nm)
$m_\perp$	14.80	(%)	β	4.81×10^{-4}	(rad)
Ψ	88	(″)	N_s	7.56×10^{7}	(cm^{-2})
$m_\parallel$	14.60	(%)			

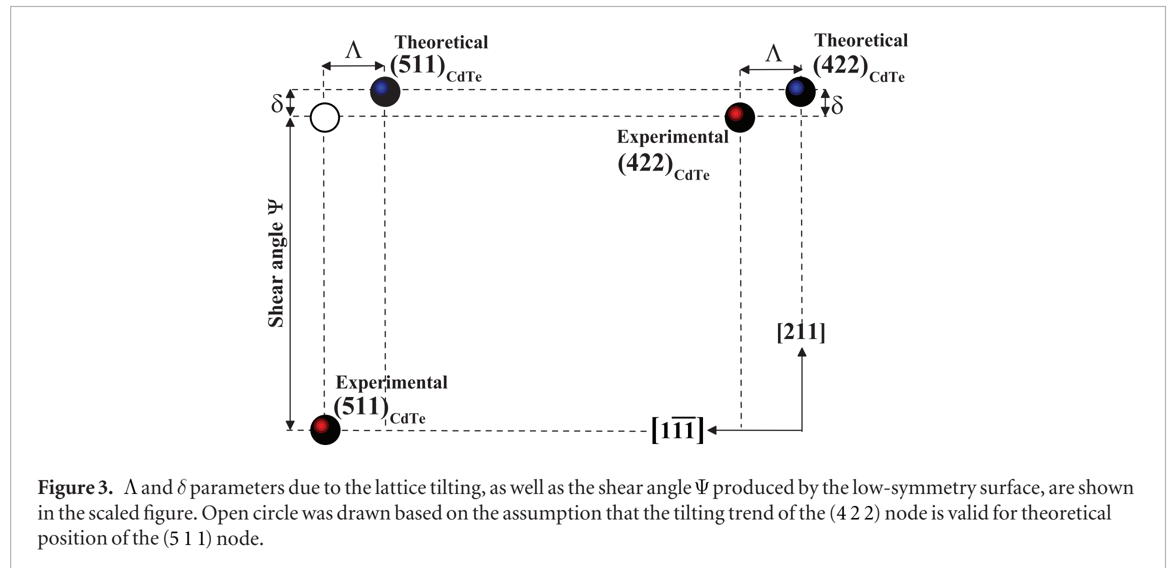

Figure 3. Λ and δ parameters due to the lattice tilting, as well as the shear angle Ψ produced by the low-symmetry surface, are shown in the scaled figure. Open circle was drawn based on the assumption that the tilting trend of the (4 2 2) node is valid for theoretical position of the (5 1 1) node.

here $a_\perp$ is the out-of-plane lattice constant of the epilayer and a_s is the lattice constant of the substrate, $|\mathbf{q}^s|$ and $|\mathbf{q}^e|$ are the scattering vector lengths of the substrate and epilayer lattices, respectively. This method may be more suitable to determine the out-of-plane lattice mismatch, if one measures the symmetric RLPs in the same diffraction plane, separately.

3.3. Shear strain

The common characteristic of the epilayers grown on the low-symmetry surfaces is the shear strain (ϵ_{xz}). The (h11) lattice planes of the epilayer are inclined under the influence of the shear strain [18]. The (5 1 1) reflection was chosen to specify the shear strain (see figure 3). The reason is that it can be easily compared to the (4 2 2) reflection by means of their Q_z coordinates, which should be identical if there is no the shear strain in the epilayer. It can be identified as follows [9]:

$$Q_z^{422} - Q_z^{511} = \pm\Psi\frac{\sqrt{6}}{a_s} \quad (3)$$

here the unit of Q_z's is $\sqrt{6}/a_s$, Ψ is the shear angle. The result in table 2 is given as the shear angle because of the fact that we described it as an inclination.

3.4. In-plane lattice mismatch

The (5 1 1) node feels simultaneously the lattice tilting and the shear strain, and as a result, these two effects change the position the (5 1 1) node (see figure 3). If we can separate the position changing caused by the lattice tilting from that caused by the shear strain, the in-plane component of the (5 1 1) node may be determined. It was observed with the help of theoretical positions that the (5 1 1) node behaves similar to the (4 2 2) node in terms of lattice tilting. The in-plane component of the (5 1 1) node was adjusted with the parameter Λ that represents the length of the tilting in the direction of the [1 $\bar{1}$ $\bar{1}$]. In other words, the parameter Λ was subtracted from the in-plane component of the experimental (5 1 1) node. As a result, the in-plane component of the epilayer lattice reaches to its initial position before the tilting. After adjustment, the lateral lattice mismatch was extracted from the following expression [17]:

$$m_\parallel = \frac{a_\parallel - a_s}{a_s} = \frac{\Delta Q_x^{511}}{Q_{x,s}^{511}} \quad (4)$$

where $a_\parallel$ is the in-plane lattice constant of CdTe, $Q_{x,s}^{511}$ is the in-plane component of the (5 1 1) node of substrate, and ΔQ_x^{511} is the difference between the in-plane component of the (5 1 1) node of the substrate and that of adjusted experimental (5 1 1) node of the epilayer.

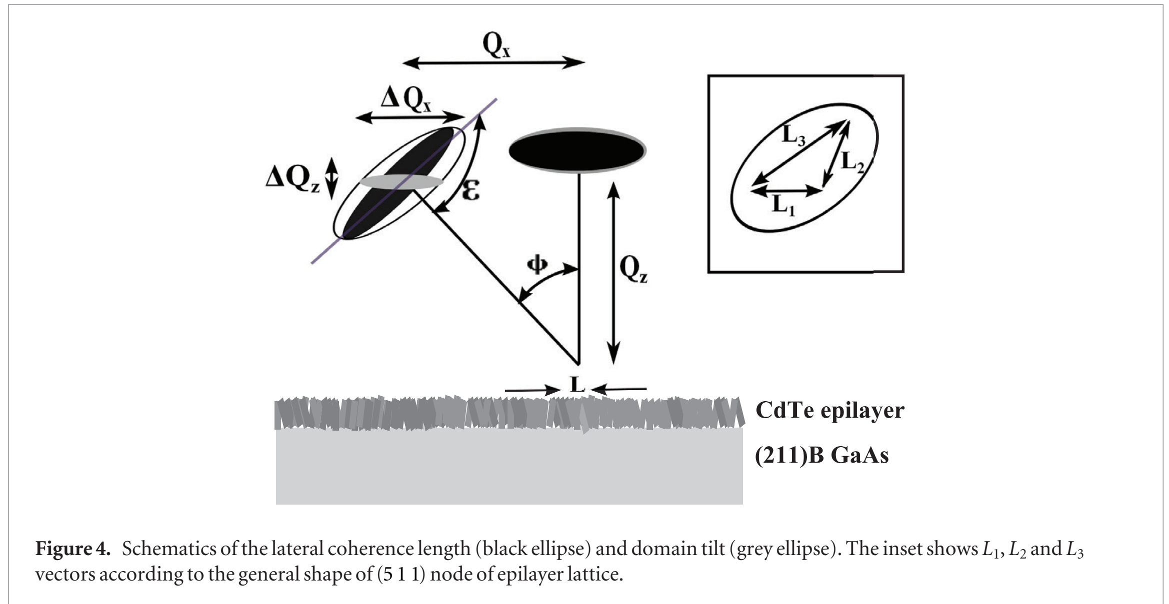

Figure 4. Schematics of the lateral coherence length (black ellipse) and domain tilt (grey ellipse). The inset shows L_1, L_2 and L_3 vectors according to the general shape of (5 1 1) node of epilayer lattice.

A very small critical thickness of 3.7 Å for the CdTe/GaAs heterostructure was calculated by a simulation based on molecular dynamics (MD) [19]. One can expect a fully relaxed epilayer for the analyzed structure. The results indicate that the compressive strain exists in the in-plane direction, while the strain becomes tensile in the growth direction because of the Poisson response of the crystal. This is nothing more than the inherent property of the low-symmetry characteristic of the structure, i.e. the shear strain. The in-plane lattice mismatch is somewhat smaller as compared to that of the out-of-plane. The divergence may be originated from the difference in elastic constants of those planes [20].

3.5. Mosaic crystal model

The relaxation process in the epilayer lattice is generally linked to the formation of a mosaic layer structure [10]. The mosaic crystal model can be described as an ensemble of the single crystalline blocks with lattice planes slightly tilted and twisted relative to each other. According to the model, the rotations of the blocks about the growth direction are associated with the domain twist, while the rotation of those blocks about the in-plane directions, i.e. either Q_x or Q_y, can be related to the domain tilt. Additionally, their sizes can be divided into the lateral and vertical lengths. Here, these terms stand for the in-plane and the out-of-plane directions, respectively [2]. These four parameters of the model can be separated to determine the TD densities which is discussed in more detail below. The ω scans, for instance, taken from at least two symmetric reflection pairs can be used to separate the lateral coherence length and the domain tilt with the help of the William-Hall plot [21].

In the case of CdTe/(2 1 1)B GaAs, the only single symmetric reflection, belonging to the epilayer lattice, may not be enough to identify the lateral coherence length and the domain tilt. However, those parameters can be extracted from the asymmetric RLP as illustrated in figure 4. We can resort to a simple geometry, as given elsewhere [22], to correlate all these parameters. They can be formulated as follows:

$$\frac{L_2}{L_1} = -\frac{\cos\varepsilon}{\cos(\phi + \varepsilon)} \tag{5}$$

$$\frac{L_3}{L_2} = \frac{\sin\phi}{\cos\varepsilon} \tag{6}$$

where $L_3 = \sqrt{\Delta Q_x^2 + \Delta Q_z^2}$, $\phi = \tan^{-1}(Q_x/Q_z)$ and $\varepsilon = \tan^{-1}(\Delta Q_x/\Delta Q_z)$. Q_x and Q_z are the coordinates of the (5 1 1) node, while ΔQ_x and ΔQ_z are the FWHMs of that node as seen in figure 4. Eventually, we need vector sums of the domain tilt perpendicular to the radial direction, L_2, and the lateral coherence length parallel to the surface plane, L_1, to relate them with L_3 as depicted in the inset. After determination of L_1 and L_2 from the above expressions, the lateral coherence length can be given as:

$$L_{\parallel} = \frac{1}{L_1} \tag{7}$$

and, the domain tilt (in radians) can be formulated as follows:

$$\beta = \frac{L_2}{\sqrt{Q_x^2 + Q_z^2}} \tag{8}$$

3.6. Screw dislocation density

The physical basis for the XRD measurements of the dislocation density relies on the characteristic parameters of the mosaic crystal model. The domain tilt and the twist can be utilized to quantify the edge-type and screw-type dislocations, respectively [23]. In our case, a Burger's vector of $\vec{b} = a/6 < 211 >$ can distort all (h11) Bragg planes such as the (5 1 1) node in the epilayer lattice. There is a relationship between the domain tilt and the screw dislocations because of the fact that the domain tilt is the measure of a quantity of the broadening around the in-plane direction as described earlier. A formula was derived to describe the relationship between the domain tilt and the screw dislocation density (N_s) [24, 25]. It can be written as follows [26]:

$$N_s = \frac{\beta^2}{4.36|\vec{b}|^2} \quad (9)$$

where β is the domain tilt and $|\vec{b}|$ is the length of the Burger's vector ($|\vec{b}| = 0.265$ nm). The screw dislocations in the CdTe crystal are more likely to lead to a higher dislocation density due to their low screw dislocation energies [27]. On the other hand, the off-axis rocking curve analysis [28] is needed to determine the domain twist, and then to find the edge dislocation density. This type of dislocation was omitted in this study due to its relatively lower density.

4. Conclusions

In summary, we have analyzed the structural characteristics of CdTe epilayer grown on high-index oriented GaAs substrate with the help of positions and FWHMs of the reciprocal lattice points. It is concluded that the lattice tilting is resulted from the out-of-plane and in-plane lattice mismatches. Moreover, the structure feels shear strain as a result of its low-symmetry surface characteristics. In addition to the lattice tilting, the shear angle gives rise to change in the position of (5 1 1) node of epilayer. The approaches presented in this letter can be also applied to similar types of heterostructures such as CdTe/(2 1 1) Si.

Acknowledgments

This study has been supported by project GEDIZ. This paper is dedicated to the memory of Professor Yusuf Selamet at Izmir Institute of Technology, who sadly passed away on Friday, August 5th, 2016.

References

[1] Fewster P F 1997 *Crit. Rev. Solid State Mater. Sci.* **22** 69
[2] Birkholz M 2006 *Thin Film Analysis by X-Ray Scattering* (Chichester: Wiley) p 297
[3] Lee S, West A, Allerman A, Waldrip K, Follstaedt D, Provencio P, Koleske D and Abernathy C 2005 *Appl. Phys. Lett.* **86** 241904
[4] Lange M, Sporken R, Mahavadi K, Faurie J, Nakamura Y and Otsuka N 1991 *Appl. Phys. Lett.* **58** 1988
[5] Ryu Y, Kang T and Kim T 2005 *J. Mater. Sci.* **40** 4699
[6] He L *et al* 2007 *J. Cryst. Growth* **301** 268
[7] Jacobs R, Markunas J, Pellegrino J, Almeida L, Groenert M, Jaime-Vasquez M, Mahadik N, Andrews C and Qadri S 2008 *J. Cryst. Growth* **310** 2960
[8] Lennon C, Almeida L, Jacobs R, Markunas J, Smith P, Arias J, Brown A and Pellegrino J 2012 *J. Electron. Mater.* **41** 2965
[9] Li M, Becker C, Gall R, Faschinger W and Landwehr G 1997 *Appl. Phys. Lett.* **71** 1822
[10] Moram M and Vickers M 2009 *Rep. Prog. Phys.* **72** 036502
[11] Arı O, Polat M, Karakaya M and Selamet Y 2015 *Phys. Status Solidi* C **12** 1211
[12] Arı O, Bilgilisoy E, Ozceri E and Selamet Y 2016 *J. Electron. Mater.* **45** 4736
[13] Bilgilisoy E, Özden S, Bakali E, Karakaya M and Selamet Y 2015 *J. Electron. Mater.* **44** 3124
[14] Karakaya M, Bilgilisoy E, Arı O and Selamet Y 2016 *AIP Adv.* **6** 075111
[15] Chauveau J M, Androussi Y, Lefebvre A, Di Persio J and Cordier Y 2003 *J. Appl. Phys.* **93** 4219
[16] Sasaki T, Tomono M and Oda N 1992 *J. Vac. Sci. Technol.* B **10** 1399
[17] Heinke H, Möller M, Hommel D and Landwehr G 1994 *J. Cryst. Growth* **135** 41
[18] Li M, Gall R, Becker C, Gerhard T, Faschinger W and Landwehr G 1997 *J. Appl. Phys.* **82** 4860
[19] Chavez J, Ward D, Wong B, Doty F, Cruz-Campa J, Nielson G, Gupta V, Zubia D, McClure J and Zhou X 2012 *Phys. Rev.* B **85** 245316
[20] Strauch D 2012 *New Data and Updates for Several III–V (including mixed crystals) and II–VI Compounds* (Berlin: Springer) pp 156–7
[21] Chierchia R, Böttcher T, Heinke H, Einfeldt S, Figge S and Hommel D 2003 *J. Appl. Phys.* **93** 8918
[22] Fewster P F 2003 *X-ray Scattering from Semiconductors* (Singapore: World Scientific)
[23] Gallinat C, Koblmüller G, Wu F and Speck J 2010 *J. Appl. Phys.* **107** 053517
[24] Gay P, Hirsch P and Kelly A 1953 *Acta Metall.* **1** 315
[25] Dunn C and Kogh E 1957 *Acta Metall.* **5** 548
[26] Ayers J 1994 *J. Cryst. Growth* **135** 71
[27] Zhou X, Ward D K, Wong B M, Doty F P and Zimmerman J A 2012 *J. Phys. Chem.* C **116** 17563
[28] Srikant V, Speck J and Clarke D 1997 *J. Appl. Phys.* **82** 4286